PROCEEDINGS OF SCIENCE

Overview of the recent results from the SND experiment at VEPP-2000 collider

M. N. Achasov,[a,b] **A. Yu. Barnyakov,**[a,b] **K. I. Beloborodov,**[a,b] **A. V. Berdyugin,**[a,b] **A. G. Bogdanchikov,**[a] **A. A. Botov,**[a] **T. V. Dimova,**[a,b] **V. P. Druzhinin,**[a,b] **V. N. Zhabin,**[a,b] **L. V. Kardapoltsev,**[a,b] **A. S. Kasaev,**[a] **A. A. Kattsin,**[a] **D. P. Kovrizhin,**[a] **A. A. Korol,**[a,b] **A. S. Kupich,**[a,b,*] **A. P. Kryukov,**[a] **N. A. Melnikova,**[a] **N. Yu. Muchnoi,**[a,b] **A. E. Obrazovsky,**[a] **A. A. Oorzhak,**[a,b] **E. V. Pakhtusova,**[a] **I. A. Polomoshnov,**[a,b] **K. V. Pugachev,**[a,b] **S. I. Serednyakov,**[a] **Z. K. Silagadze,**[a,b] **I. K. Surin,**[a] **Yu. V. Usov,**[a] **A. G. Kharlamov,**[a,b] **D. A. Shtol**[a] **and V. V. Zhulanov**[a]

[a] *Budker Institute of Nuclear Physics of Siberian Branch Russian Academy of Sciences, 11, Acad. Lavrentieva Pr., Novosibirsk, 630090 Russian Federation*

[b] *Department of theoretical physics, Novosibirsk State University, 1, Pirogova str., Novosibirsk, 630090, Russia*

E-mail: A.S.Kupich@inp.nsk.su

Recent results on the study of e^+e^- annihilation into hadrons at $\sqrt{s} < 2$ GeV obtained in the SND experiment at the VEPP-2000 collider are presented. We announce the results of high precision measurements of the $e^+e^- \to \pi^+\pi^-$ and $e^+e^- \to K_S K_L$ cross sections, and analyses of the processes $e^+e^- \to n\bar{n}$, $e^+e^- \to \pi^+\pi^-\pi^0$, $e^+e^- \to \omega\eta\pi^0$, $e^+e^- \to \pi^0\gamma$, and $e^+e^- \to \pi^0\pi^0\gamma$. Also, we present preliminary results on the study of the two photon process $e^+e^- \to e^+e^-\eta$ and measurement of the inclusive hadronic cross section at 1.8 GeV $< \sqrt{s} < 2$ GeV.

The 21st International Conference on Hadron Spectroscopy and Structure (HADRON2025)
27 - 31 March, 2025
Osaka University, Japan

*Speaker

 ISSN 1824-8039 . Published by SISSA Medialab.

PoS(HADRON2025)027

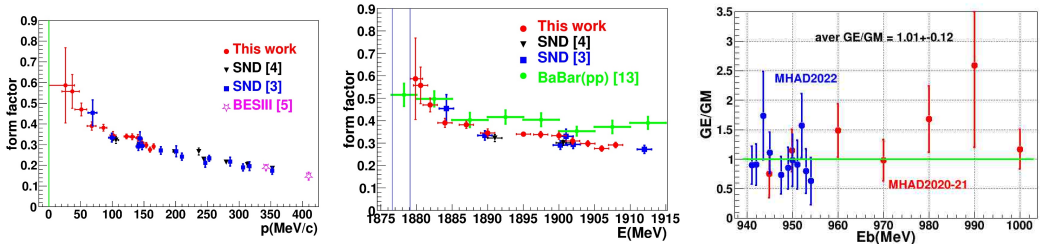

Figure 1: Left panel: The SND result on the neutron effective form factor (F_n), compared with the previous SND results [5, 6] (black and blue dots) and $F_n(p_n)$ measured by BES-III [7] (purple stars). Central panel: measured $F_n(\sqrt{s})$, compared with the earlier SND results (black and blue dots) and the proton form factor measured by BABAR [8] (green dots). Right panel: The preliminary SND results on the G_E/G_M ratio measurement for different experimental runs.

1. Introduction

SND [1–4] is the universal nonmagnetic detector consisting of a nine-layer drift chamber, 9 threshold aerogel Cherenkov counters, a three-layer spherical electromagnetic calorimeter (EMC) with 1640 NaI(Tl) crystals, and a muon system.

SND data taking at the VEPP-2000 e^+e^- collider started in 2010. At this point a data sample with an integrated luminosity of about 1 fb^{-1} has been collected in the 0.3–2.0 GeV energy range.

Main physics task of the SND experiment is the study of all possible processes of e^+e^- annihilation into hadrons at $\sqrt{s} < 2$ GeV. In particular, these measurements are used to obtain the total hadronic cross section needed for Standard Model calculation of the anomalous magnetic moment of muon and running electromagnetic coupling constant (complementary to lattice QCD calculations). A detailed study of the dynamics of exclusive processes is also performed to probe the hadronic structure. In this report we present SND results on the processes $e^+e^- \to \pi^+\pi^-$, $e^+e^- \to K_S K_L$, $e^+e^- \to n\bar{n}$, $e^+e^- \to \pi^+\pi^-\pi^0$, $e^+e^- \to \omega\eta\pi^0$, $e^+e^- \to \pi^0\gamma$, $e^+e^- \to \pi^0\pi^0\gamma$ and $e^+e^- \to e^+e^-\eta$.

2. Study of the $e^+e^- \to n\bar{n}$

The neutron produces a very low energy deposition in the calorimeter. Therefore, its signal is not used in this analysis. The antineutron annihilates inside the EMC, producing pions, protons and neutrons. EMC allows to measure time of the $\bar{n}$ annihilation with an accuracy of about 1 ns. The time distribution for selected events consists of the nearly uniform cosmic-ray distribution, the distribution for the beam-induced and physical backgrounds, which is peaked near zero, and a wide $n\bar{n}$ distribution, which is shifted relative to other e^+e^- annihilation events due to small $\bar{n}$ velocity. Number of $e^+e^- \to n\bar{n}$ events is determined from the fit to data with the sum of the three distributions. Fig. 1 (left, central) depict the effective form factor of the neutron measured in this work in comparison with the results of previous measurements by SND [5, 6] and BES-III [7]. Analysis of the angular distributions allows to obtain the ratio of the electric and magnetic form factors (G_E/G_M). Preliminary results of the G_E/G_M measurements are shown in Fig. 1 (right), and they are consistent with unity.

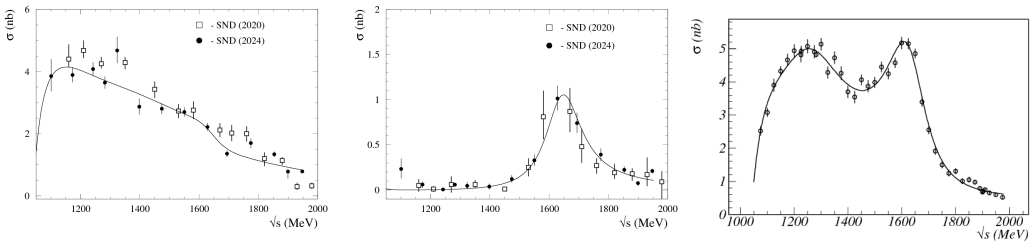

Figure 2: Cross sections for the $\rho(770)\pi$ (left panel) and $\rho(1450)\pi$ (central panel) mechanisms and total $e^+e^- \to \pi^+\pi^-\pi^0$ cross section (right panel). Empty dots depict previously published SND measurement [9], solid curves are the VMD fit results.

3. $e^+e^- \to \pi^+\pi^-\pi^0$

Events with two non-collinear tracks and two photons are selected. For selected events, the Dalitz plot analysis is performed. It's observed that the $\omega(1650)$ resonance decays mainly via the $\rho(1450)\pi$ mechanism, while $\omega(1420)$ via the $\rho(770)\pi$. The $\omega(1650)$ width in the channel is 148±13 MeV, and consistent with the other decay modes. The cross sections for $\rho(770)\pi$ and $\rho(1450)\pi$ mechanisms, and total 3π cross section are presented in Fig. 2.

Below 1.05 GeV the $e^+e^- \to \pi^+\pi^-\pi^0$ cross section is dominated by the contributions of the ω and φ resonances. The most precise measurement (1.3%) was carried out in the BABAR experiment [10], and we plan to perform measurement with a comparable accuracy. Our advantage is the precise measurement of beam energy. From the VMD fit we expect to extract the most precise measurements of the B($\varphi \to 3\pi$), B($\rho \to 3\pi$), $\psi(\rho-\omega)$, $\psi(\varphi-\omega)$, m_ω and Γ_ω.

4. Study of the $e^+e^- \to K_S K_L$ process

Events with $K_s \to \pi^0\pi^0$ decay are selected using kinematic fit for events with at least 4 photons in the final state. Two models are used to describe the cross section: simple Vector Meson Dominance model and the one with interactions of the K_S and K_L in the final state (FSI). The latter provides significantly better fit quality: χ^2/ndf=13.7/14 against 23.7/14 for the pure VMD model (Fig. 3), thus showing 3.2 σ significance for FSI. The SND at VEPP-2M and CMD-2 measurements agree with our measurement [11] within the systematic errors (0.9% at the maximum of the φ). The difference with the CMD-3 measurement is 1.7 σ.

5. $e^+e^- \to \pi^0\pi^0\gamma$ and $e^+e^- \to \pi^0\gamma$ analysis

Events with 5 photons and no charged particles in the final state are selected. Then the kinematic fit to the $\pi^0\pi^0\gamma$ hypothesis is performed. There are two mechanisms for $\pi^0\pi^0\gamma$ final state: with vector-pseudoscalar intermediate state ($\omega\pi^0$, $\rho\pi^0$) and radiative decays ($f_0(500)\gamma$, $f_0(980)\gamma$, $f_2(1270)\gamma$, $f_0(1370)\gamma$). Dalitz plot fit allows to calculate total cross sections of all radiative processes (Fig. 4, right). The contribution of radiative decays has greater than 5 σ significance and shows a resonant structure at 1.7 GeV. At this point of the analysis adding hypothetical $\rho(1250)$ to the model greatly improves fit of the cross section for the dominant $\omega\pi^0$ mechanism (Fig. 4, left).

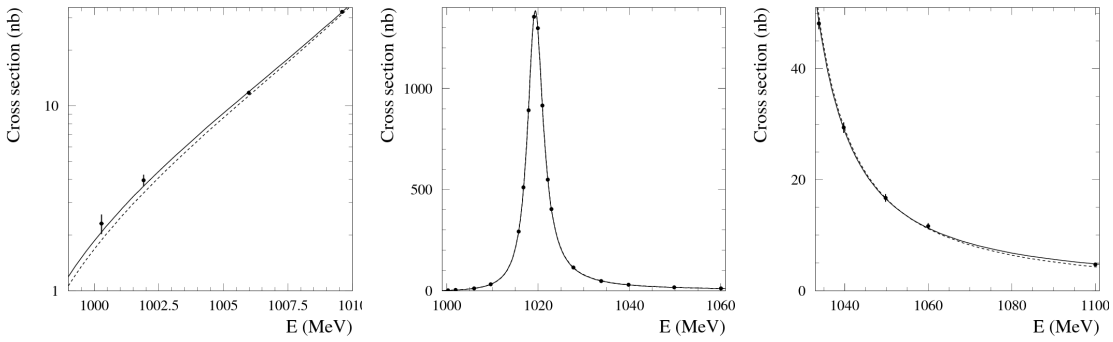

Figure 3: The $e^+e^- \to K_S K_L$ cross section in the φ-meson region (central panel), near threshold (left panel) and higher energies (right panel). Solid lines shows the fit result with the VMD+FSI model, dashed lines are the simple VMD model.

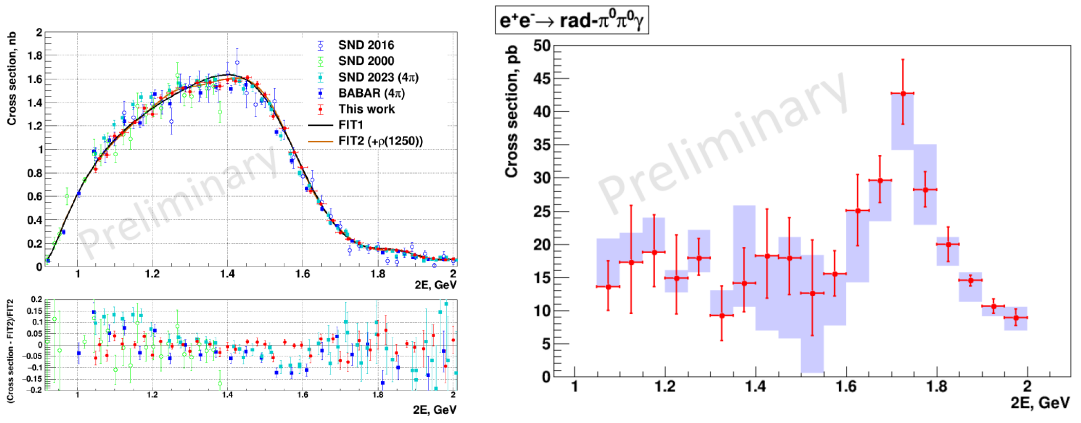

Figure 4: Left panel: fit of the measured $e^+e^- \to \omega\pi^0$ cross section, comparing to previous SND [12] and BABAR [13] results. Right panel: total cross sections of all radiative processes, red dots are result of the fit with a baseline model, shaded areas depict model uncertainty.

The number of the $e^+e^- \to \pi^0\gamma$ events is derived from the fit of the invariant mass of two less energetic photons after kinematic fit in $e^+e^- \to 3\gamma$ hypothesis. Result of the new measurement of the $B(\varphi \to \pi^0\gamma)$ is 7–15% higher, comparing to the previous measurements [14].

6. Inclusive measurement of charged non-collinear hadronic cross section in the 1.8-2.0 GeV region

The measured cross sections also include contributions from the neutral hadronic processes with η and K_s decaying into the states with charged particles. Events containing two central, non-collinear tracks are selected, with additional cuts applied to reduce beam-induced background contribution. Efficiency is calculated using Monte Carlo simulation (MC) of the 42 exclusive hadronic processes, mixed according to the cross sections, previously measured in SND, CMD-3, BABAR and BES experiments. Main QED background is suppressed by the cuts on energy deposition in the different layers of EMC, depicted in Fig. 5 (left). The cosmic background contribution is estimated from

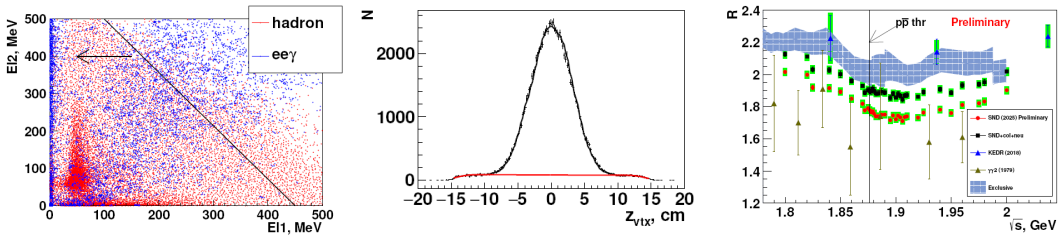

Figure 5: Left panel: distribution of the energy deposition for hadronic processes (red) and QED background (blue). Central panel: example of a fit of the vertex z-coordinate distribution, red curve shows contribution of the beam-induced background. Right panel: preliminary results of the inclusive hadronic cross section measurement by SND, comparing to previous inclusive measurements [15, 16], shaded area depicts sum of all known exclusive hadronic cross sections.

EMC time distribution, under assumption that it is uniform for cosmic events. MC is used to calculate number of the expexted QED background events. Residual beam-induced background is subtracted via fit of the vertex z-coordinate distribution (Fig. 5, center), with shape of the signal determined by selected $e^+e^- \to \pi^+\pi^-\pi^0\pi^0$ events and polynomial function used for background. In order to calculate total hadronic cross section, previously measured cross sections of the neutral ($\eta\pi^0\gamma$, $\pi^0\pi^0\gamma$, $\pi^0\gamma$, $\eta\eta\gamma$, K_SK_L etc.) and collinear (K^+K^- , $\pi^+\pi^-$ and $p\bar{p}$) hadronic processes are added (Fig. 5, right).

7. $e^+e^- \to e^+e^-\eta$ and $e^+e^- \to \omega\eta\pi^0$

Two–photon events with $\eta \to 3\pi^0$ decay are selected using kinematic fit for events with more than 5 photons in the final state. Machine learning is used to suppress beam-induced background. Contribution from the $ep \to ep\eta$ background is estimated using number of events with $|R_{BDT}|$ <0.4 and R_{BDT} distribution from MC of the $ep \to ep\eta$ (Fig. 6, left). Residual hadronic background is calculated from MC of the known processes of the e^+e^- annihilation. Results of the cross section measurement are consistent with theoretical predictions [17] (Fig. 6, center). The obtained $\Gamma_{\eta\to\gamma\gamma}$=0.527±0.03 keV is in agreement with KLOE result [18].

Analysis of the $e^+e^- \to \omega\eta\pi^0 \to \pi^+\pi^-\pi^0\pi^0\eta \to \pi^+\pi^-6\gamma$ is based on 443 pb^{-1} data collected by SND. Below 1.9 GeV our measurement shows systematic deviation from the BABAR result [19]. There is about 50% difference at 1.975 GeV (Fig. 6, right).

8. High precision $e^+e^- \to \pi^+\pi^-$ cross section measurement

The $e^+e^- \to \pi^+\pi^-$ cross section measurements are playing a significant role in calculations of (g-2) of the muon. Current analysis is based on 2018 data (47 pb^{-1}) collected below 1 GeV. Latest version of the BabaYaga-NLO generator [20] is now implemented in MC. $e^+e^- \to \pi^+\pi^-$ and $e^+e^- \to e^+e^-$ events are separated with the machine learning methods using information about energy depositions in the EMC crystals. Integrated luminosity for each energy point is calculated from the number of $e^+e^- \to e^+e^-$ events. Efficiency for each process is derived from MC events, and then corrected to match experimental data. To reduce these corrections multiple modifications

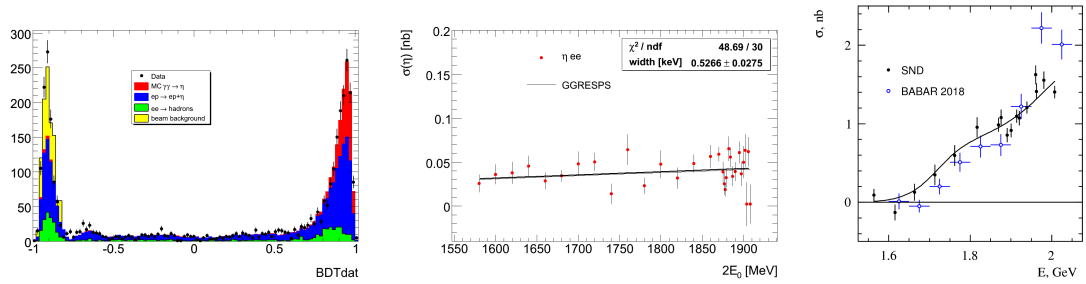

Figure 6: Left panel: fit of the discriminator response distribution (R_{BDT}), red and blue histograms are distributions for simulated $e^+e^- \to e^+e^-\eta$ and $ep \to ep\eta$ events respectively, yellow one is a distribution for beam-induced background, green histogram – residual hadronic background. Central panel: fit of the measured $e^+e^- \to e^+e^-\eta$ cross section (thick line) and theoretical prediction [17] (thin line). Right panel: fit of the measured $e^+e^- \to \pi^+\pi^-\pi^0\pi^0\eta$ cross section, blue dots – BABAR results [19].

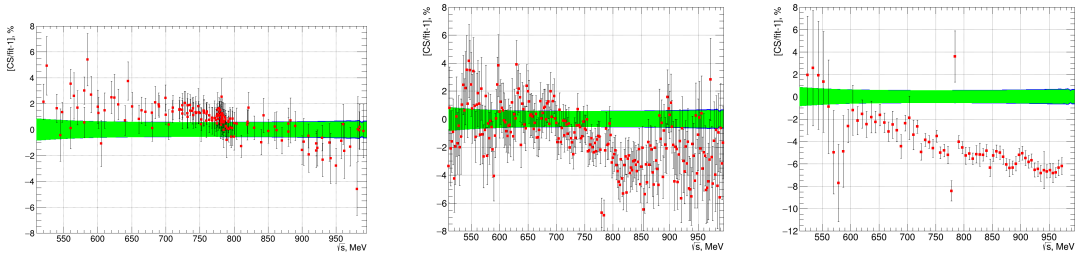

Figure 7: The relative difference between the CMD-3 [22] (left panel), BABAR [23] (central panel) and KLOE [24] (right panel) $e^+e^- \to \pi^+\pi^-$ results and the fit of preliminary SND data. The blue and green bands represent the total and systematic uncertainties of the SND fit respectively.

of the MC and reconstruction software have been performed. With radiative and beam energy spread corrections, the Born cross section is calculated. The systematic uncertainty is estimated to be 0.6-0.8%. The new measurement is 2% higher than the previously published SND results [21] (based on 2013 dataset). After reanalysis with a new version of software, the 2013 SND data are consistent with our new results. One of the possible explanations: shortcomings of the old version of reconstruction algorithms resulted in unaccounted loss of the pion tracks. Comparisons with previous measurements [22–24] are depicted in Fig. 7. Our results are consistent with BaBar measurement [23] at $\sqrt{s} < 0.78$ GeV, and 3% greater at higher energies (Fig. 7, central). Deviation from CMD-3 results [22] is no greater than 1.3% (Fig. 7, left). Combined KLOE measurements [24] are incompatible with the new SND data (Fig. 7, right).

References

[1] M. N. Achasov et al., *First experience with SND calorimeter at VEPP-2000 collider*, *Nucl. Instrum. Methods Phys. Res., Sect. A* **598** (2009) 31.

[2] V. M. Aulchenko et al., *SND tracking system–Tests with cosmic muons*, *Nucl. Instrum. Methods Phys. Res., Sect. A* **598** (2009) 102.

[3] Y. Barnyakov et al., *Particle identification system based on dense aerogel for SND detector at VEPP-2000 collider,* *JINST* **9** (2014) C09023.

[4] V. M. Aulchenko et al., *DAQ and electronics for SND at VEPP-2000—First test results*, *Nucl. Instrum. Methods Phys. Res., Sect. A* **598** (2009) 340.

[5] M. N. Achasov et al., *Measuring the Neutron Timelike Electromagnetic Form Factor with the SND Detector,* *Phys. Atomic Nucl.* **86** (2023) No.6, p.1165.

[6] M. N. Achasov et al., *Cross Section of the Process $e^+e^- \to n\bar{n}$ near the Threshold,* *Phys. Atomic Nucl.* **87** (2024) No.5, p.604.

[7] M. Ablikim et al., *Measurements of the Electric and Magnetic Form Factors of the Neutron for Timelike Momentum Transfer,* *Phys. Rev. Lett.* **130** (2023) 151905.

[8] J. P. Lees, V. Poireau, V. Tisserand et. al., *Study of $e^+e^- \to p\bar{p}$ via initial-state radiation at BABAR,* *Phys. Rev. D* **87** (2013) 092005.

[9] M. N. Achasov et al., *Study of dynamics of the process $e^+e^- \to \pi^+\pi^-\pi^0$ in the energy range 1.15–2.00 GeV,* *Eur. Phys. J. C* **80** (2020) 993.

[10] G. Vasseur, *Measurement of $e^+e^- \to \pi^+\pi^-\pi^0$ at BABAR and calculation of $(g-2)_\mu$,* *Nucl. and Part. Phys. Proc.* **324–329** (2023) pp. 119-124.

[11] M. N. Achasov et al., *Measurement of the $e^+e^- \to K_S K_L$ cross section near the $\phi(1020)$ resonance with the SND detector,* *Phys. Rev. D* **110** (2024) 072001.

[12] M. N. Achasov et al., *Study of the process $e^+e^- \to \omega\pi^0 \to \pi^+\pi^-\pi^0\pi^0$ in the energy range 1.05–2.00 GeV with SND,* *Phys. Rev. D* **108** (2023) 092012.

[13] J. P. Lees, V. Poireau, V. Tisserand et al., *Measurement of the $e^+e^- \to \pi^+\pi^-\pi^0\pi^0$ cross section using initial-state radiation at BABAR,* *Phys. Rev. D* **96** (2017) 092009.

[14] M. N. Achasov et al., *Study of the reaction $e^+e^- \to \pi^0\gamma$ with the SND detector at the VEPP-2M collider,* *Phys. Rev. D* **93** (2016) 092001.

[15] V. V. Anashin, O. V. Anchugov, V. M. Aulchenko et al., *Precise measurement of Ruds and R between 1.84 and 3.72 GeV at the KEDR detector,* *Phys. Let. B* **788** (2019) pp. 42-51.

[16] C. Bacci, G. De Zorzi et al., *Total cross section for hadronic production by e^+e^- annihilation in the total cm energy range 1.42–3.09 GeV,* *Phys. Let. B* **86** (1979) pp. 234-238.

[17] V. M. Budnev, I. F. Ginzburg, G. V. Meledin, V. G. Serbo, *The two-photon particle production mechanism. Physical problems. Applications. Equivalent photon approximation,* *Phys. Rep.* **15** (1975) Is. 4 pp. 181-282.

[18] D. Babusci, D. Badoni et al., *Measurement of η meson production in $\gamma\gamma$ interactions and $\Gamma(\eta \to \gamma\gamma)$ with the KLOE detector,* *J. High Energ. Phys.* **2013** (2013) 119.

[19] J. P. Lees, V. Poireau, V. Tisserand et al., *Study of the reactions $e^+e^- \to \pi^+\pi^-\pi^0\pi^0\pi^0$ and $e^+e^- \to \pi^+\pi^-\pi^0\pi^0\eta$ at center-of-mass energies from threshold to 4.35 GeV using initial-state radiation,* Phys. Rev. D **98** (2018) 112015.

[20] E. Budassi, C. M. Carloni Calame, M. Ghilardi et al., *Pion pair production in e^+e^- annihilation at next-to-leading order matched to Parton Shower,* J. High Energ. Phys. **2025** (2025) 196.

[21] M. N. Achasov et al., *Measurement of the $e^+e^- \to \pi^+\pi^-$ process cross section with the SND detector at the VEPP-2000 collider in the energy region $0.525 < \sqrt{s} < 0.883$ GeV,* J. High Energ. Phys. **2021** (2021) 113.

[22] F. V. Ignatov et al., *Measurement of the $e^+e^- \to \pi^+\pi^-$ cross section from threshold to 1.2 GeV with the CMD-3 detector*, Phys. Rev. D **109** (2024) 112002.

[23] J. P. Lees, V. Poireau, V. Tisserand et al.,*Precise measurement of the $e^+e^- \to \pi^+\pi^-(\gamma)$ cross section with the initial-state radiation method at BABAR*, Phys. Rev. D **86** (2012) 032013.

[24] A. Anastasi, D. Babusci et al., *Combination of KLOE $\sigma(e^+e^- \to \pi^+\pi^-\gamma(\gamma))$ measurements and determination of $a_\mu^{\pi^+\pi^-}$ in the energy range $0.1 < s < 0.95\ GeV^2$,* J. High Energ. Phys. **2018** (2018) 173